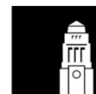

UNIVERSITY OF LEEDS

This is a repository copy of *Proteomic profiling of the large-vessel vasculitis spectrum identifies shared signatures of innate immune activation and stromal remodelling*.

White Rose Research Online URL for this paper:
https://eprints.whiterose.ac.uk/221574/

Version: Accepted Version

Article:

Maughan, R.T., MacDonald-Dunlop, E., Haroon-Rashid, L. et al. (13 more authors) (2025) Proteomic profiling of the large-vessel vasculitis spectrum identifies shared signatures of innate immune activation and stromal remodelling. Arthritis & Rheumatology. ISSN 2326-5191

https://doi.org/10.1002/art.43110

Reuse
This article is distributed under the terms of the Creative Commons Attribution (CC BY) licence. This licence allows you to distribute, remix, tweak, and build upon the work, even commercially, as long as you credit the authors for the original work. More information and the full terms of the licence here: https://creativecommons.org/licenses/

Takedown
If you consider content in White Rose Research Online to be in breach of UK law, please notify us by emailing eprints@whiterose.ac.uk including the URL of the record and the reason for the withdrawal request.

eprints@whiterose.ac.uk
https://eprints.whiterose.ac.uk/

1 **Proteomic profiling of the large-vessel vasculitis spectrum identifies shared**
2 **signatures of innate immune activation and stromal remodelling**
3
4 **Short Title:**
5 Proteomic profiling of large-vessel vasculitis
6
7 **Authors:**
8 Robert T. Maughan PhD[1,2]*, Erin MacDonald-Dunlop PhD[1]*, Lubna Haroon-Rashid BSc[3],
9 Louise Sorensen PhD[3,4], Natalie Chaddock PhD[3], Shauna Masters RGN[5], Andrew Porter PhD
10 MRCP[2], Marta Peverelli MSc[2], Charis Pericleous PhD[2], Andrew Hutchings MSc[6], James
11 Robinson PhD[3], Taryn Youngstein MD MRCP[2], Raashid A. Luqmani DM FRCP[5], Justin C.
12 Mason PhD FRCP[2]‡†, Ann W. Morgan PhD FRCP[3,4]‡, James E. Peters PhD MRCP[1]‡
13
14 1. Department of Immunology and inflammation, Imperial College London, UK.
15 2. National Heart and Lung Institute, Imperial College London, UK
16 3. Leeds Institute of Cardiovascular and Metabolic Medicine, University of Leeds, Leeds, UK
17 4. NIHR Leeds Biomedical Research Centre, Leeds Teaching Hospitals NHS Trust, Leeds, UK.
18 5. Nuffield Department of Orthopaedics, Rheumatology and Musculoskeletal Science (NDORMs),
19 University of Oxford, Oxford, UK
20 6. Department of Health Services Research and Policy, London School of Hygiene & Tropical
21 Medicine, UK
22 *joint first authors, ‡ joint senior authors, † deceased
23
24 **Correspondence to:**
25 r.maughan@imperial.ac.uk, a.w.morgan@leeds.ac.uk, or j.peters@imperial.ac.uk
26

Sources of Funding

This study was funded in part by the Medical Research Council (MRC) “Treatment According to Response in Giant cEll arTeritis” (TARGET) Partnership award (MR/N011775/1), Medical Research Foundation (MRF-042-0001-RG-PETE-C0839), Vasculitis UK (V2105), MRC Confidence in Concept (Leeds), the NIHR Imperial Biomedical Research Centre (BRC), and the NIHR Leeds BRC (NIHR203331). The TABUL study was funded via an NIHR Heath Technology Assessment grant. N.C. was supported by an MRC DiMen award. C.P. was supported by Versus Arthritis (Career Development Fellowship, 21223) and Imperial College -Wellcome Trust Institutional Strategic Support Fund (ISSF). J.E.P. is supported by a Medical Research Foundation Fellowship (MRF-057-0003-RG-PETE-C0799). A.W.M. is an NIHR Senior Investigator (NIHR202395) and supported by the NIHR Leeds BRC and was previously supported by the NIHR Leeds MedTech and Invitro Diagnostics Co-operative and MRC TARGET Partnership grant. The views expressed are those of the authors and not necessarily those of the NIHR or the Department of Health and Social Care.

Disclosures

J.E.P. has received travel and accommodation expenses to speak at Olink-sponsored academic meetings (none in the last 5 years). C.P. is a recipient of a research grant from Galapagos BV; unrelated to this study. A.W.M. previously received a research grant from Roche PLC, for unrelated work, and has undertaken consultancy or received honoraria for speaking at educational events on behalf of her institution from AstraZeneca, Roche and Vifor in the last 5 years. R.A.L has served on advisory boards for GSK and Roche; has received assistance to attend meetings from CSL Vifor; has received grants from Roche, Celgene/BMS and CSL Vifor, and has participated in clinical trials for Roche, GSK, Novartis, and InflaRx.

50 # Abstract

51 **Background**: Takayasu arteritis (TAK) and giant cell arteritis (GCA), the most common forms
52 of large-vessel vasculitis (LVV), can result in serious morbidity. Understanding the molecular
53 basis of LVV should aid in developing better biomarkers and treatments.

54 **Methods:** Plasma proteomic profiling of 184 proteins was performed in two cohorts. Cohort 1
55 included patients with established TAK (n=96) and large-vessel GCA (LV-GCA, n=35) in
56 addition to healthy control participants (HCs, n=35). Cohort 2 comprised patients presenting
57 acutely with possible cranial-GCA in whom the diagnosis was subsequently confirmed (C-
58 GCA, n=150) or excluded (Not C-GCA, n=89). Proteomic findings were compared to published
59 transcriptomic data from LVV-affected arteries.

60 **Results:** In Cohort 1, comparison to HCs revealed 52 differentially abundant proteins (DAPs)
61 in TAK and 72 in LV-GCA. Within-case analyses identified 16 and 18 disease activity-
62 associated proteins in TAK and LV-GCA, respectively. In Cohort 2, comparing C-GCA versus
63 Not C-GCA revealed 31 DAPs. Analysis within C-GCA cases suggested the presence of
64 distinct endotypes, with more pronounced proteomic changes in the biopsy-proven subgroup.
65 Cross-comparison of TAK, LV-GCA and biopsy-proven C-GCA revealed highly similar plasma
66 proteomic profiles, with 26 shared DAPs including IL6, monocyte/macrophage related proteins
67 (CCL7, CSF1), tissue remodelling proteins (TIMP1, TNC) and novel associations (TNFSF14,
68 IL7R). Plasma proteomic findings reflected LVV arterial phenotype; for 42% of DAPs, the
69 corresponding gene was differentially expressed in tissue.

70 **Conclusions:** These findings suggest shared pathobiology across the LVV spectrum
71 involving innate immunity, lymphocyte homeostasis and tissue remodelling. Network-based
72 analyses highlighted immune-stromal crosstalk and identified novel therapeutic targets (e.g.
73 TNFSF14).

74

Introduction

Takayasu arteritis (TAK) and giant cell arteritis (GCA), the most common forms of large-vessel vasculitis (LVV) in adults, are characterised by granulomatous arterial inflammation. Progressive damage to arterial walls typically results in stenotic remodelling with consequent tissue ischaemia and manifestations such as sight loss, stroke, myocardial infarction and limb claudication[1]. Despite phenotypic similarities, TAK and GCA have different demographics, particularly age of onset, and, to a lesser extent, they affect different arterial territories. TAK affects the aorta and its major branches, while classically GCA has been described as involving the cranial arteries (C-GCA) such as the temporal artery. However, following advances in non-invasive vascular imaging techniques, it became clear that the aorta and other large vessels are frequently affected in GCA, and some patients have a large vessel-type presentation (LV-GCA) with non-specific constitutional symptoms and/or limb claudication similar to TAK[2,3]. Frequent large vessel involvement in GCA and similar histopathological changes has led to debate regarding whether TAK and GCA represent varying manifestations of the same disease[4,5]. This question has important implications for drug development and clinical trial design. However, such comparisons are currently limited by an incomplete understanding of the pathogenic underpinnings of these diseases and a lack of comparative molecular data across LVV phenotypes.

There are several important challenges in the clinical management of TAK and GCA. Both initial diagnosis and recognition of relapse may be delayed and are made more difficult by a lack of effective biomarkers[6]. Blood tests such as C-reactive protein (CRP) lack specificity while vascular imaging can be insensitive, particularly in glucocorticoid-treated patients, and impractical for frequent serial monitoring[7,8]. In the era before widespread access to ultrasound scans (USS), the diagnosis of C-GCA was confirmed by performing a temporal artery biopsy (TAB). While considered the "gold standard" diagnostic test, the presence of skip lesions may lead to false negative results. A negative biopsy therefore does not exclude the diagnosis of GCA. Progress in the treatment of LVV, particularly the development of targeted biologic therapy, lags behind that of other rheumatic diseases. Accordingly, there is overreliance on long-term glucocorticoids to maintain disease control with resulting iatrogenic harm[9,10]. Thus, there is a need for better biomarkers and novel therapeutics to improve patient outcomes.

Proteomic profiling has the potential to address these challenges[11]. Proteins are the effector molecules of most biological functions and the targets of most drugs. Given the proximity of arterial tissue to the circulation, blood-based proteomics is likely to be informative in LVV.

111 Specifically, we hypothesised that the levels of inflammation- and cardiovascular-related
112 proteins would provide a read-out of disease activity and arterial pathobiology in LVV patients
113 and enable evaluation of molecular similarities and differences between GCA and TAK. To
114 this end, we performed proteomic profiling of 184 circulating proteins in two independent
115 cohorts that included 281 patients with TAK, LV-GCA or C-GCA. We identified protein
116 signatures associated with each LVV type and with disease activity. Cross-disease
117 comparison revealed a striking similarity between the proteomic profiles of active LVV types.
118 Our data indicate the shared dysregulation of innate immune and tissue remodelling pathways
119 and highlight the potential for therapeutics targeting immune-stromal cross-talk.

120 Methods

121

122 Cohort 1 study participants

123 Patients with TAK or LV-GCA were recruited from the Hammersmith Hospital (Imperial College
124 Healthcare NHS Trust, UK) between 2013 and 2020. TAK patients fulfilled EULAR/ACR 2022
125 classification criteria[12] and all had typical patterns of arterial involvement in radiological
126 assessments. LV-GCA patients were >50 years at onset with radiological evidence of LVV, as
127 defined previously[13]. Three LV-GCA patients had concurrent temporal artery involvement
128 (confirmed by temporal artery USS and/or TAB). Healthy control participants (HCs) were
129 recruited locally from hospital and college staff and had no history of inflammatory or
130 cardiovascular disease. Citrate blood samples were centrifuged at 1000G for 10 minutes
131 within 4 hours of venepuncture and plasma was stored at -80°C until use. Disease activity was
132 assessed using the Indian Takayasu Clinical Activity Score (ITAS2010) for TAK[14] and the
133 National Institutes of Health (NIH) score for LV-GCA[15]. Active disease was defined as
134 ITAS2010 score ≥ 1 or ITAS-CRP ≥ 2 for TAK and NIH score ≥ 2 for LV-GCA. All inactive
135 cases were retrospectively confirmed to be relapse free for 1 year following sample collection.
136 For the purpose of further investigation within inactive TAK cases, 'durable clinical remission'
137 was defined as: (i) absence of all signs, symptoms, and laboratory features attributable to
138 active TAK (as per EULAR definition[16]); (ii) absence of arterial progression on serial vascular
139 imaging; (iii) criteria i and ii sustained for past 3 years; and (iv) successful cessation of all
140 immunosuppressive treatment. Patients and HCs provided written informed consent, and
141 samples were collected as a sub-collection registered with the Imperial College Healthcare
142 Tissue Bank (licence: 12275; National Research Ethics Service approval 17/WA/0161).
143

Cohort 2 study participants

The Temporal Artery Biopsy vs ULtrasound in Diagnosis of GCA (TABUL) was an international, multicentre, prospective study which compared the sensitivity and specificity of temporal artery ultrasound to biopsy in 381 patients with suspected C-GCA[17] [ClinicalTrials.gov: NCT00974883]. Reference diagnosis of C-GCA or Not C-GCA at 6 months was based on a combination of baseline signs and symptoms, blood tests, TAB, fulfilment of ACR 1990 GCA classification criteria, clinical course during the follow-up period, final consultant diagnoses and verification by an expert review panel, as described previously[17].

Cranial ischaemic complications were defined as permanent ocular or non-ocular conditions at presentation. Ocular complications: anterior ischaemic optic neuropathy, branch retinal artery occlusion, cilioretinal artery occlusion, cranial nerve palsy (III, IV or V), central retinal artery occlusion, posterior ischaemic optic neuropathy relative afferent pupillary defect; irreversible visual loss; irreversible visual field defect; irreversible ocular motility or irreversible diplopia. Non-ocular cranial complications: scalp necrosis; tongue necrosis; cerebrovascular accident at presentation considered secondary to GCA). Polymyalgic symptoms at presentation are also reported but do not represent a confirmed diagnosis of polymyalgia rheumatica.

Citrated blood samples collected as soon as feasible after starting glucocorticoid treatment (median 2 days, IQR 1-4) and were centrifuged at 2500 G for 15 minutes within 1.5 hours of collection and plasma was stored at -80°C until use. Due to funding constraints and biosample availability, we performed Olink proteomic assays on 239 patient samples out of the 381 patients recruited to TABUL. We included all available samples from patients with a diagnosis of C-GCA. We selected a subset of sex and age (+/- 5 years) matched Not C-GCA cases such that the ratio of C-GCA to Not C-GCA was approximately 2:1. As part of the study design, we selected an equal proportion of cases with cranial ischaemic complications in the C-GCA group as in the Not C-GCA group. Overall study approval was granted by the Berkshire Research Ethics Committee (09/H0505/132) and approval was also granted at local participating clinical sites.

Proteomic analysis

184 proteins were measured by proximity extension assay using two Olink Target panels, ‘Inflammation 1’ and ‘Cardiometabolic’ at the Leeds Immunogenomics Facility, University of Leeds. In order to provide a succinct and standardised nomenclature, we report proteins by the symbols of the genes encoding them (see **Supplementary Data 1** for a full list of proteins and associated full names and accession numbers). Cohort 1 and 2 samples were processed

181 and analysed independently, but proteomic measurements were performed in the same
182 facility. We designed assay plates such that samples were balanced across plates according
183 to disease grouping and disease activity status, with randomisation to determine well position
184 within plates. Proteomic data were normalised using standard Olink workflows, which includes
185 inter-plate normalisation, to produce measures of relative protein abundance ('NPX') (log_2
186 scale). For visualisation, we transformed to Z-scores (mean=0, SD=1). Due to a technical fault
187 with a PCR machine during the running of one plate on the Inflammation 1 panel for Cohort 2,
188 it was necessary to re-run this plate as a separate batch. Principal component analysis (PCA)
189 revealed a batch effect, with samples from this plate separated from samples on the other
190 three plates run as part of the first batch. We therefore adjusted for this batch effect for proteins
191 measured on the Inflammation 1 panel in Cohort 2, using batch (a binary variable) as a
192 covariate in linear model based differential abundance analyses. For situations requiring
193 batch-correction outside of differential abundance testing (e.g. visualisation of protein levels
194 using violin plots and heatmaps and network analyses), the residuals from the linear model
195 (in Wilkinson notation) NPX ~ Batch were used to generate batch-corrected protein values.
196 Further PCA of these residuals confirmed that the batch effect had been removed. The
197 residuals were then converted to Z scores prior to visualisation or other downstream analyses.
198 Cardiometabolic panels for Cohort 1 were not affected by this issue and were analysed as a
199 single batch.
200
201 Proteins with >75% of samples below the lower limit of detection were removed resulting in
202 158 and 167 protein measurements for Cohort 1 and 2, respectively. Sample-level quality
203 control (QC) was performed using internal assay controls, boxplots of relative protein
204 abundance values and PCA for outlier detection. In Cohort 1, three samples (1 HC and 2 TAK)
205 were excluded from Inflammation panel measurements due to amplification failures. In Cohort
206 2, fifteen samples (9 C-GCA and 6 Not C-GCA) were excluded from Inflammation panel and
207 3 (all C-GCA) from the Cardiometabolic panel measurements due to amplification failures and
208 flagged status in internal QC checks. Where possible all available data was analysed (e.g.
209 differential abundance analyses) but some analyses (e.g. hierarchical clustering, PCA,
210 multiple linear regression versus clinical parameters) necessitated using only complete data.
211
212 Differential protein abundance was performed using linear models (*lm* function in R). For a
213 given protein, protein abundance was regressed on disease status (encoded as 0 or 1). The
214 beta coefficient for the disease status term represents the estimated log_2 fold change in the
215 protein level between groups under comparison. For example, for the analysis of TAK versus
216 HCs, the regression model was NPX ~ D, where NPX was log_2 protein level (continuous
217 variable) and D was a binary variable, encoded as 0 for HC and 1 for TAK. Correction for

218 multiple testing (multiple proteins) was performed using the Benjamini-Hochberg method
219 (p.adjust function, method= "BH") and an adjusted P-value of < 0.05 (i.e. false discovery rate
220 < 5%) was defined as significant.
221

222 **Protein annotation**

223 The 184 proteins measured were highly enriched for pathways related to immune function and
224 cardiovascular homeostasis as demonstrated by Reactome pathway over-representation
225 analysis (**Supplementary Data 2**). Due to this enrichment, proteins were manually classified
226 as "Cytokine Related", "Growth Factor Related", "Chemokine, Other Immune/Inflammatory
227 related protein", "Extracellular matrix Related" or "Other Function" to facilitate the annotation
228 of differential abundance results. This was done using a combination of public resources
229 including Gene Ontology terms, pathway and functional databases. The full list of proteins and
230 associated classifications is provided in **Supplementary Data 1**.
231

232 **Network analysis**

233 The protein-protein interaction network between differentially abundant proteins was
234 constructed using high confidence interactions (confidence ≤ 0.9) sourced from STRING[18]. No
235 additional filtering of interactions was performed. The protein co-expression network of
236 differentially abundant proteins was created using inter-protein correlation of abundance
237 values. Node edges were defined as Pearson $r \geq 0.6$. Cohort 1 (TAK and LV-GCA) and Cohort
238 2 (C-GCA) networks were computed individually and then intersected so that only correlations
239 present in both networks feature in the final network. Both networks were plotted using the
240 igraph package in R[19].
241

242 **Tissue expression of differentially abundant proteins**

243 GTEx bulk RNA-seq tissue expression data was accessed as median transcript per million
244 values per tissue[20]. Data pre-processing included: removal of sex-specific organ data (i.e.
245 cervix, breast, vagina, testis, fallopian tubes), removal of purified cell data (e.g. cultured
246 fibroblasts) and where there were multiple sample types per tissue group (e.g. Artery-Coronary
247 or Artery-Aorta) the highest expression value was used for that tissue type. Enhanced tissue
248 expression of differentially abundant proteins was defined as >4 fold higher than the average
249 expression in other tissues as done previously by the Human Protein Atlas[21].
250

251 **RNA-seq analysis of LVV arterial tissue**

252 A previous study compared the transcriptomic profile of inflammatory and non-inflammatory
253 aortic aneurysms using bulk RNA-seq[22]. Gene-level count data was accessed and filtered for
254 cases of inflammatory aneurysm associated with GCA (n=8) for comparison with non-

255 inflammatory cases (n=25). Data was normalised, genes with low expression were removed
256 and groups were compared using the standard edgeR package methodology[23]. Differentially
257 expressed (DE) genes were defined using Benjamini Hochberg adjusted $P < 0.05$. DE genes
258 were then compared with LVV-associated plasma proteins with regards to overlap and
259 Pearson correlation of $\log_2$ fold change in each disease.

260

261 **Supervised learning**

262 Predictive models to develop disease activity biomarkers in TAK and diagnostic markers in C-
263 GCA using the *glmnet*[24] and *caret*[25] R packages. For these analyses data were split into
264 Training and Test sets. Modelling fitting was performed on the Training Set using 5-fold cross-
265 validation and performance then evaluated in the Test set. Full details are provided in the
266 **Supplementary Methods**.

267

268 **Other analyses**

269 Details of additional analyses are provided in **Supplementary Information File**.

270

271 **Data and Code availability**

272 The post QC proteomic data are available from figshare:
273 https://doi.org/10.6084/m9.figshare.26928211.v1
274 The raw proteomic data and the R code for QC and differential abundance analysis are
275 available from Github https://github.com/r-maughan/LVV_Olink

276

277 ## Results

278

279 To identify proteins associated with LVV and to evaluate the presence of shared or distinct
280 molecular signatures across TAK, LV-GCA and C-GCA, we measured plasma levels of 184
281 inflammation- and cardiovascular-related proteins (**Supplementary Data 1**) in two
282 independent cohorts using the Olink Target antibody-based proximity extension assay (**Figure**
283 **1**). To provide a standardised nomenclature, we report proteins using the non-italicised HUGO
284 gene symbol of the encoding gene.

285

286 **Shared plasma proteomic profiles in TAK and LV-GCA**

287 Cohort 1 included 96 TAK patients, 35 LV-GCA patients and 35 healthy controls (HCs)
288 (**Supplementary Table 1**). Patient characteristics were typical for TAK and LV-GCA with
289 regards to age and sex, with younger onset and greater female:male ratio in TAK. HCs were
290 well matched in terms of demographics to the TAK patients. LV-GCA patients were older and

291 had a higher proportion of individuals of White European ancestry. The patient samples
292 analysed encompassed a broad range of disease activity, disease duration and treatment
293 status, particularly in TAK where sample size was greater. Patients with active disease tended
294 to have shorter disease durations and were receiving higher glucocorticoid doses, as might
295 be expected (**Supplementary Data 3**). In Cohort 1, 158 proteins (86%) passed QC
296 parameters (**Methods**) and were available for analysis.
297
298 Comparison of proteomic profiles between TAK patients and HCs identified 52 differentially
299 abundant proteins (DAP), with 42 upregulated and 10 downregulated (**Figure 2A,**
300 **Supplementary Data 4**). Cross-referencing of our results to those of a previous study[26] which
301 used a different proteomic platform demonstrated that many of our proteomic associations
302 were novel (**Figure S1**, **Supplementary Data 4**). We next compared LV-GCA to HCs,
303 revealing 72 DAP, with 60 increased and 12 decreased (**Figure 2B, Supplementary Data 5**).
304 The proteomic changes in TAK and LV-GCA in comparison to HCs were highly similar; 40
305 proteins were significantly altered in both diseases and 85% of all proteins had directionally
306 concordant changes compared to HCs (**Figure 2C&D**). Proteomic similarity of TAK and LV-
307 GCA was also reflected in principal component analysis (PCA), with TAK and LV-GCA
308 clustering together and separated from HCs (**Figure S2A**).
309
310 As expected, many upregulated proteins in TAK and LV-GCA indicated immune activation
311 including cytokines, chemokines, and growth factors (**Figure S2B**). Plasma IL6, the pleiotropic
312 cytokine of known importance to LVV pathogenesis[13], was significantly upregulated in both
313 TAK and LV-GCA (**Figure 2E**), together with liver-derived inflammatory proteins such as SAA4
314 and FCN2. Prominent innate immune involvement in both TAK and LV-GCA was indicated by
315 increased levels of neutrophil-derived proteins (S100A12, LCN2, DEFA1) and
316 monocyte/macrophage activation and chemotactic factors (CSF1, CCL3, CCL5, CCL7,
317 CCL14). Plasma levels of TNF (tumour necrosis factor), IL12B and IFNG were not significantly
318 altered despite previous links to TAK pathogenesis[27]. In contrast, we observed large increases
319 in OSM (oncostatin M) and TNFSF14 (LIGHT), cytokines not previously associated with LVV
320 (**Figure 2E**). In addition to the dysregulation of immune-related proteins, we observed the
321 upregulation of proteins with functions related to the extracellular matrix (TIMP1, MMP1,
322 CST3, TNC), fibrosis (TGFB1) and angiogenesis (VEGFA, HGF, ANG, COL18A1) in both
323 diseases, likely reflecting a signature of arterial injury and remodelling. Six proteins were
324 consistently downregulated in both diseases, including IL7R, KIT, TNXB and THBS4 (both
325 extracellular matrix (ECM) related glycoproteins), DPP4 (a glucose metabolism and T-cell
326 activation factor) and CR2 (the complement C3d receptor).
327

328 To evaluate whether there were disease-specific effects, we performed a direct comparison
329 of TAK versus LV-GCA, which revealed 6 significant DAP (**Supplementary Data 6**).
330 Visualising the relative abundance of these proteins in each group demonstrated that the
331 dysregulation of these proteins appeared to be LV-GCA specific (**Figure S3A**). For example,
332 in LV-GCA, but not TAK, CXCL9, CCL11 and CA3 levels were elevated compared to HCs.
333 Similarly, CR2 and TNFSF11 (RANKL) were significantly reduced in LV-GCA but not in TAK.
334 Changes specific to TAK were less prominent, with no proteins that had significant changes
335 in TAK versus both HCs and LV-GCA. However, we observed that FGF23 and IL17A were
336 significantly increased in TAK compared to HCs but were not significantly increased in LV-
337 GCA versus HC (**Figure S3B**).
338

339 **Signatures of active disease in TAK and LV-GCA patients**

340 To identify proteins associated with disease activity in TAK and LV-GCA, we next compared
341 the proteomic profile of active and inactive patients within each disease. In TAK, 16 proteins
342 were significantly altered in active disease, with 11 upregulated and 5 downregulated (**Figure**
343 **3A**, **Supplementary Data 7**). Upregulated proteins included neutrophil-related factors
344 (S100A12, CXCL5 CXCL1), liver-derived proteins (SAA4, CFHR5), ECM components (TNC,
345 NID1, CRTAC1, COMP) and angiogenic factors (VEGFA, ANG), indicating innate immune
346 activation and vascular remodelling (**Figure 3B**). To corroborate the results of the active
347 versus inactive patient analysis and identify proteins whose levels vary with the degree of
348 disease activity, we tested for association with the numerical ITAS2010 disease activity
349 score[14]. 8 of the 158 proteins measured were significantly correlated (adjusted $P<0.05$) with
350 the ITAS2010 score (**Figure S4A&C**), and 7 of these 8 were differentially abundant in the
351 active versus inactive analysis.
352

353 Assessment of disease activity in TAK is currently based on the evaluation of clinical features,
354 imaging, and clinical laboratory measures of inflammation, particularly CRP levels. However,
355 CRP lacks both sensitivity and specificity for active TAK[7]. In keeping with this, 20 active TAK
356 patients had normal CRP levels (<5mg/L). We found that 6 proteins (NID1, TNC, S100A12,
357 CD274 (sPD-L1), DEFA1 and DPP4) were more strongly correlated with ITAS2010 than CRP
358 (**Figure S4**). Motivated by this finding, we formally evaluated whether we could develop a
359 multi-marker protein signature using supervised learning to improve classification of disease
360 activity (**Supplementary Material**). Using LASSO regression, we generated a 10-protein
361 signature which outperformed CRP (AUC 0.8 versus 0.72 respectively; **Figure S5A&B**).
362 However, a simpler two-protein logistic regression model comprising CRP and COMP
363 performed even better (AUC 0.9; **Figure S5C**), demonstrating proof-of-principle that even the

364 addition of a single protein could provide improved and clinically tractable biomarker-based
365 assessment of disease activity in TAK.
366
367 In LV-GCA, 18 proteins were significantly associated with active disease, with 17 increased
368 and 1 decreased (**Figure 3A**, **Supplementary Data 8**). Although two proteins (CFHR5 and
369 VEGFA) were increased in active disease in both LV-GCA and TAK, the LV-GCA activity
370 signature was mostly distinct to that of TAK (**Figure 3A&C**). A more prominent acute phase
371 response was evident in active LV-GCA compared to TAK with large increases in IL6 and
372 multiple liver-derived inflammatory proteins (MBL2, ST6GAL1, C2) (**Figure 3D**). There were
373 also differences in the chemokines and other immunoregulatory proteins affected; CXCL5 and
374 CXCL1 levels were not significantly changed in active LV-GCA (**Figure 3E**) but there were
375 increases in the monocyte-attracting chemokines (CCL7, CCL14, CCL23) and the T-cell
376 recruitment and activation factors (CCL18, GNLY, TIMD4). Lastly, there were activity-
377 associated increases in remodelling associated proteins TIMP1, COL18A1 and NRP1 in LV-
378 GCA but not TAK.
379
380 To determine whether proteomic differences persist despite clinically quiescent disease, we
381 compared inactive TAK and LV-GCA patients to HC participants. This analysis identified 22
382 and 61 DAP in inactive TAK and LV-GCA, respectively, with 18 common to both diseases
383 (**Figure S6A-C**, **Supplementary Data 9-10**). Examples of proteins which remained elevated
384 in inactive disease include OSM, S100A12, TNFSF14 and AXIN1 (**Figure S6D**). Importantly,
385 these proteins remained chronically elevated regardless of disease duration (**Figure S6E**),
386 even in TAK patients who had withdrawn all treatment following durable clinical remission
387 (**Figure S6D**; median time off treatment 2 years [inter-quartile range, IQR: 1.5-5.1], further
388 details in **Supplementary Data 11**). Thus, our data indicate that some proteomic changes
389 observed in TAK and LV-GCA patients represent persistent molecular derangements which
390 do not normalise with clinical remission.
391
392 **Biopsy proven C-GCA has a distinct proteomic endotype**
393 We next performed proteomic profiling of an independent cohort (Cohort 2) of 239 patients
394 presenting acutely with possible C-GCA, recruited to the TABUL study[17]. Blood samples were
395 taken rapidly following initiation of high dose glucocorticoids; median treatment duration was
396 2 days (IQR: 1-4). All patients underwent both temporal artery biopsy (TAB) and ultrasound
397 sonography (USS) and a diagnosis of C-GCA was subsequently confirmed or excluded (Not
398 C-GCA). Patient characteristics were typical for suspected C-GCA, with the majority of cases
399 being over 60 years old (87.4%), female (72%) and having White European ancestry (99.3%)

400 (**Supplementary Table 2**). Of patients diagnosed with C-GCA, 56 (37.3%) had a positive TAB,
401 78 (52%) had an abnormal USS and 53 (35.3%) were negative for both TAB and USS where
402 diagnosis was based on clinical features. Compared to Not C-GCA patients, C-GCA patients
403 were slightly older (median age 4 years greater) and had higher ESR, CRP and platelet levels
404 (**Supplementary Table 2**). Proteomic profiling was performed using the same Olink platform.
405 167 proteins (91%) passed QC parameters and data from a minimum of 225 patients were
406 available for analysis (**Methods**).
407
408 Proteomic comparison of C-GCA patients (n=150) to Not C-GCA cases (n=89) revealed 31
409 DAP (**Figure 4A**, **Supplementary Data 12**). Further investigation revealed heterogeneity of
410 these protein profiles within C-GCA patients and that differences compared to Not C-GCA
411 cases were mostly driven by the TAB positive (TAB+) C-GCA patient subset (**Supplementary**
412 **Methods**, **Figure S7**). In analyses stratified by TAB result, comparison of TAB+ C-GCA (n=56)
413 to Not C-GCA identified 62 DAP (**Figure 4B**, **Supplementary Data 13**), while only 1 DAP was
414 identified in the TAB negative (TAB-) C-GCA (n=89) versus Not C-GCA comparison
415 (**Supplementary Data 14**). The increase in significant associations when limiting to biopsy-
416 proven cases despite reduction in sample size and hence statistical power indicates that TAB+
417 C-GCA is enriched for proteomic signal, and that the TAB- group were diluting this signal in
418 the analysis of all C-CGA versus Not C-GCA. Comparison of the estimated $\log_2$ fold changes
419 ($\log_2$FC) and protein abundances from the TAB+ and TAB- stratified analyses confirmed larger
420 magnitudes of effect in the former (**Figure 4D & 4F**). We additionally found that TAB+ C-GCA
421 patients had higher levels of CRP, ESR, platelets and presence of polymyalgic symptoms
422 compared to TAB- C-GCA patients (**Figure 4C & Supplementary Data 15**). Moreover, PCA
423 of all proteins assayed indicated separation of TAB+ from TAB- C-GCA patients (**Figure S7C**).
424 Together, these findings indicate that C-GCA can be stratified into biologically and clinically
425 distinct subsets by TAB result.
426
427 Further exploration of TAB- patients with hierarchical clustering revealed that while the large
428 majority did not share the TAB+ associated signature, 18 TAB- patients were similar to TAB+
429 patients (**Figure S8**). However, this pattern had no significant association with demographic
430 or clinical parameters. Relatedly, the comparison of C-GCA TAB- patients who had abnormal
431 USS (N=36) to Not C-GCA cases did not identify any significant proteins. Together, these
432 results suggest that TAB rather than USS positivity more closely reflects the proteomic
433 phenotype.
434
435 The 62 proteins associated with TAB+ C-GCA patients suggest both innate and adaptive
436 immune activation with dysregulation of cytokines, growth factors, chemokines and other

437 immune-related proteins (**Figure 4E**). In a previous proteomic study[28], five of these proteins
438 were identified as significantly altered in C-GCA (**Figure S9** & **Supplementary Data 13**).
439 Similar to TAK and LV-GCA, many proteins involved in innate immune function were
440 upregulated including acute phase response mediators (IL6, MBL2, SAA4, CFHR5,
441 ST6GAL1) and factors involved in neutrophil and monocyte migration and activation (CXCL1,
442 CCL14, CCL7, S100A12, CSF1). Several chemokines involved in T- and B-cell recruitment
443 were also increased (CXCL9, CXCL10, CXCL11, CCL18) together with altered levels of
444 lymphocyte survival and proliferation factors (increased IL7, decreased: IL7R, KITLG,
445 TNFSF11). In addition, increases in ECM (MMP1, TIMP1, TNC, LTBP2), fibrosis (TGFB1) and
446 angiogenesis-related proteins (VEGFA, HGF, NRP1) were indicative of vascular remodelling.
447 The downregulated proteins with the lowest p-values were SERPINA5 and DPP4 (**Figure 4F**).
448 In secondary analyses, we did not identify any proteins that were significantly associated with
449 cranial ischaemic complications or polymyalgic symptoms within C-GCA patients when
450 analysed both as a single group and when separated by TAB result.
451

452 **Supervised learning to identify protein-based diagnostics for C-GCA**

453 There are no specific diagnostic blood tests for C-GCA. While ESR and CRP are typically
454 elevated, they are non-specific. For example, CRP was elevated (>5mg/L) in 69% of Not C-
455 GCA cases in this study. We therefore tested whether a blood-based protein or proteomic
456 biomarker could aid diagnosis of C-GCA, randomly splitting the data into training and test sets
457 (**Supplementary Material**). Using logistic regression models, the best predictive univariate
458 markers for biopsy-proven C-GCA were CXCL9, DPP4 and SERPINA5 (**Figure S10A,**
459 **Supplementary Table 3**). Despite having one of the larger estimated LFCs in the differential
460 abundance analyses (**Figure 4A-B**), IL6 was less effective as a predictor (**Supplementary**
461 **Table 3)**. We then explored whether predictive performance could be enhanced through a
462 more sophisticated multivariate modelling approach. We supplied all proteins measured as
463 input variables and trained a model using LASSO regression (which performs variable
464 selection) and cross-validation. This resulted in an 11-protein model which provided improved
465 diagnostic performance compared to the univariate models (accuracy 0.87, AUC 0.94) (**Figure**
466 **S10B, Supplementary Tables 3-4**). The most important features in the LASSO model were
467 CXCL9, DPP4 and SERPINA5 (**Figure S10B)**, consistent with the findings of the univariate
468 logistic regression analyses.
469

470 **Correlated proteomic changes in active TAK, LV-GCA and biopsy-proven C-GCA with**
471 **IL6 and VEGFA identified as key hub proteins**
472 We next explored similarities and differences in the plasma proteomic signatures associated
473 with each form of LVV. We considered the possibility that our results might be impacted by
474 differences in study design. In Cohort 2, C-GCA patients were sampled with active disease at
475 the time of diagnosis, whereas in Cohort 1, patients were sampled during both active and
476 inactive disease over a range of disease durations. To mitigate against this, we re-analysed
477 Cohort 1 restricting case samples to active disease only. These analyses revealed 68 and 69
478 differentially abundant proteins for active TAK versus HCs and active LV-GCA versus HCs
479 respectively, of which the majority had also been significantly altered in the corresponding
480 previous analyses using all cases (80.9% and 81.6% respectively, **Supplementary Data 16-**
481 **17**). We then compared the results of these TAK and LV-GCA analyses to the proteomic
482 associations identified in the TAB+ C-GCA versus Not C-GCA comparison in Cohort 2.
483
484 112 DAP were identified in one or more LVV type (subsequently referred to as LVV-associated
485 proteins, **Figure 5A, Supplementary Data 18**). Directional changes were highly similar with
486 74 (66.1%) having concordant changes (**Figure 5B**) and significant correlation between both
487 TAK and LV-GCA profiles with that of TAB+ C-GCA (Pearson *r* 0.49 and *r* 0.69, respectively,
488 both $P<0.0001$). Twenty-six proteins (23.2%) were dysregulated in all three diseases and 33
489 proteins (29.5%) were dysregulated in two. Of the 26 shared DAP, all had directionally
490 concordant changes, including 20 upregulated and 6 downregulated proteins. We define these
491 26 proteins as the 'pan-LVV signature' (**Supplementary Data 18**). Upregulated proteins
492 included IL6, acute phase proteins (SAA4, CFHR5, ST6GAL1), monocyte and neutrophil
493 factors (S100A12, CSF1), monocyte and lymphocyte chemokines (CCL5, CCL7, CCL3,
494 CCL18, CCL23) and TNFSF14. Also increased were proteins related to arterial remodelling
495 including VEGFA, HGF, MMP1, TIMP1 and the ECM glycoprotein Tenascin C (TNC).
496 Decreases included IL7R, KIT and KITLG, each involved in lymphocyte differentiation and
497 proliferation, DPP4, CR2 and TNXB (another ECM tenascin).
498
499 Using the GTEx tissue transcriptome database[20], we explored the global tissue expression
500 profile of each LVV-associated protein, defining enhanced expression as >4 fold higher than
501 average tissue level as per Human Protein Atlas methodology[21]. 83 (74.1%) had enhanced
502 expression in ≥1 tissue. The most represented tissues were liver, spleen and whole blood
503 (**Figure S11**). 11 proteins had enhanced arterial expression including TNC, TIMP1, COL18A1
504 and TNFRSF11B (OPG), thereby indicating the possibility of blood-based measurement of
505 arterial biomarkers in LVV.
506

507 To infer relationships between proteins, we constructed two networks using the 74 proteins
508 with concordant changes using i) annotated protein-protein interactions (String-db[18]) (**Figure**
509 **5C**) and ii) co-expression (Pearson $r \geq 0.6$) (**Figure 5D**). The network of annotated interactions
510 identified IL6 and IL10 as the central hubs with connections to proteins with distinct functions
511 including chemotaxis (e.g. CCL5, CCL3), angiogenesis (e.g. VEGFA, HGF) and tissue
512 remodelling (e.g. MMP1, TIMP1, TGFB1). In the network constructed using protein co-
513 expression data, TIMP1 and VEGFA displayed even greater connectivity, appearing as central
514 nodes with edges connecting both to other remodelling-related proteins (e.g. COL18A1,
515 NRP1) and multiple immune-associated proteins (e.g. CSF1, TNFSF14, CCL14). These
516 networks indicate the coordinated regulation of immune and vascular remodelling processes,
517 highlighting immune-stromal cross-talk in LVV.
518
519 The most prominent inter-disease differences diseases were between TAK and LV-GCA
520 profiles compared to TAB+ C-GCA (**Figure 5A**). In particular, the large increases in EIF4EBP1
521 and AXIN1 observed in TAK and LV-GCA were not seen in C-GCA. Similarly, increases in the
522 neutrophil proteins DEFA1 and LCN2 were observed exclusively in TAK and LV-GCA (**Figure**
523 **5E**). There were also differences between LV-GCA and TAB+ C-GCA profiles compared to
524 TAK which indicate some degree of divergence between diseases. For example, increases in
525 CXCL9 and TIMD4 were seen only in the GCA groups while decreases in the ECM-related
526 proteins COMP and THBS4 were only found in TAK (**Figure 5F**).
527

528 **Plasma proteomic signatures reflect LVV arterial tissue phenotype**

529 Plasma proteins arise not only from blood cells but also from a wide range of tissues and
530 organs, including the vasculature which is in direct contact with the blood. We therefore sought
531 to evaluate whether changes in patient plasma (**Figure 5A**) reflect the phenotype of arterial
532 tissue affected by LVV. Using bulk RNA-seq data from a study which compared surgically
533 resected aortic tissue of LV-GCA to non-inflammatory aortic aneurysms (NI-AA)[22], we found
534 that for 47 (42%) of the LVV-associated plasma proteins, the corresponding gene was
535 differentially expressed in LVV arterial tissue (**Figure 6A, Supplementary Data 19**).
536 Moreover, the $\log_2$FCs of these 47 plasma proteins correlated with the $\log_2$FC of the
537 corresponding gene in LVV tissue versus NI-AA (**Figure 6B**), and 28 (59.6%) had directionally
538 concordant changes across the transcriptomic analysis of LVV arterial tissue and the plasma
539 proteomic analyses of all the 3 LVV types.
540
541 Using the blueprint and GTEx bulk RNA-seq datasets[20,29], we explored the cell-type and
542 arterial expression profile of the 47 genes/proteins dysregulated in both plasma and arterial

543 tissue (**Figure S12A**). Macrophage and neutrophil expressed genes/proteins made up the
544 largest subset (34%); this included CCL7, CSF1, CXCL9 and CDCP1 which were increased
545 in both tissue and plasma (**Figure 6C**). Genes/proteins expressed by non-immune stromal
546 cells such as TNC, MMP1, TIMP1 and NRP1 were also prominent (**Figure 6D**). This latter
547 cluster was enriched for genes of high arterial expression (GTEx) and could be useful as
548 markers of arterial remodelling. The remainder were lymphocyte-derived (**Figure 6E**) or had
549 mixed expression profiles. Of note, despite the significant decreases in plasma protein DPP4,
550 CR2 and IL7R in LVV, the expression of the corresponding genes was significantly increased
551 in LVV arterial tissue (**Figure S12B**), emphasising that there may be directionally discordant
552 effects between different tissue compartments and/or between intracellular mRNA expression
553 and plasma protein levels. Overall, these findings indicate that plasma proteomic signatures
554 can reflect aspects of LVV tissue phenotype and could provide a valuable non-invasive read-
555 out of pathogenic processes occurring in diseased arteries.
556
557 ## Discussion
558
559 TAK and GCA are currently classified as separate diseases[12,30] but some investigators have
560 proposed that they could represent varying manifestations of the same disease spectrum[4,5].
561 This debate has largely focused on phenotypic similarities, reflecting patterns of arterial injury[3].
562 Genome-wide association studies reveal differences in the genetic risk factors that associated
563 with TAK or GCA diagnosis[31]. However, a key unanswered question is whether the molecular
564 effector pathways acting in these diseases are shared or distinct. This information is critical
565 for the rational selection of new therapeutic strategies that target specific proteins.
566
567 Here, we address this by comparing the plasma proteomic profile of TAK, LV-GCA and C-
568 GCA. In 281 patients with LVV, we measured 184 inflammation- and vascular-associated
569 proteins to characterise the plasma proteome of each major LVV type and evaluate changes
570 associated with disease activity states. We found that the proteomic profiles associated with
571 active TAK, LV-GCA and biopsy-proven C-GCA were similar and identified a 26-protein 'pan-
572 LVV' signature common to all three groups. This signature primarily included proteins of
573 immunological function, but it also comprised proteins arising from or acting on the stroma,
574 indicative of arterial injury and/or repair. Some of these proteins have well-established roles
575 in LVV (e.g. IL6 and VEGFA)[13,27], but others have not been previously linked to LVV.
576
577 The signature reflected prominent innate immune activation, particularly with increases in
578 several proteins related to monocyte and macrophage function. Importantly, co-expression

579 analysis revealed coordinated regulation of such proteins (e.g. CSF1, CCL18, CCL14) with
580 multiple proteins involved in tissue remodelling (e.g. VEGFA, TIMP1 and TGFB1) thereby
581 highlighting innate immune-stromal crosstalk in LVV. This is consistent with recent reports
582 implicating pro-fibrotic macrophage subsets in the fibrotic and stenotic remodelling of arteries
583 in TAK and GCA, cell types that are less affected by current treatments[32,33]. These findings
584 underscore the importance of macrophages in TAK and GCA pathogenesis and illustrate the
585 need for markers and therapeutics which target macrophages beyond pro-inflammatory
586 functions alone.
587
588 We also observed evidence for adaptive immune involvement, with changes in lymphocyte-
589 related proteins like IL7R and TNFSF14. Plasma IL7R was decreased in all LVV groups
590 irrespective of disease activity status. Its ligand IL7 was also significantly increased in TAK
591 and C-GCA. IL7 is essential for T-cell development and homeostasis whilst soluble (sIL7R)
592 potentiates IL7 activity by enhancing bioavailability[34]. The pattern observed is similar to
593 findings in ANCA-associated vasculitis and tuberculosis infection but contrasts with
594 rheumatoid arthritis and lupus where sIL7R levels are increased[35–37]. Interestingly, the mRNA
595 expression of IL7R was increased in the transcriptomic analysis of LV-GCA aortitis and a
596 recent study reported that IL7R expressing T-cells are involved in the persistence of vasculitic
597 lesions in a mouse chimeric model [38]. Decreased IL7R in LVV patient plasma may therefore
598 reflect the recruitment of specific T-cell subsets from the circulation to vasculitic lesions. As
599 another example, TNFSF14 (LIGHT) was prominently elevated. TNFSF14 acts as a T-cell
600 costimulatory factor and triggers T-cell activation and proliferation[39]. TNFSF14 promotes
601 systemic immunopathology, as demonstrated by transgenic animals with constitutive
602 TNFSF14 expression in T-cells[40]. Moreover, TNFSF14 can also act on non-haematopoietic
603 structural cells including fibroblasts, endothelial and smooth muscle cells to drive tissue
604 fibrosis[41]. Consistent with this, our co-expression network analysis identified an edge
605 connecting TNFSF14 to VEGFA, a central hub node. Current treatment strategies in LVV are
606 limited to suppression of inflammation and do not target fibrosis directly. Thus, TNSF14
607 antagonism may be a novel therapeutic approach in LVV that provides dual targeting of both
608 the immune response and the consequent stromal reaction.
609
610 Lastly, the signature included tissue remodelling proteins expressed by immune cells (e.g.
611 VEGFA) or stromal cells (e.g. TNC, TIMP1, MMP1); the latter may represent useful markers
612 of arterial damage independent of inflammation. Increased plasma TNC in LVV is relevant
613 given its enrichment in normal arteries and increased expression in arteries affected by LVV.
614 TNC is an ECM protein primarily expressed by fibroblasts at sites of tissue damage where it

615 supports repair. It gained interest as a candidate marker of vascular injury, but its levels are
616 also elevated in other disease states[42]. Although this lack of specificity to LVV may preclude
617 its use as a diagnostic marker, TNC and other ECM proteins could be useful for monitoring
618 arterial injury during follow-up and should be evaluated in longitudinal studies.
619
620 Despite the overall similarity in LVV proteomic profiles, we identified differences which suggest
621 some immunological divergence between diseases. For example, the chemokine CXCL9 was
622 higher in LV-GCA and C-GCA compared to TAK. CXCL9 is produced by macrophages and
623 other cell types in response to interferon-gamma and typically reflects activation of the Th1
624 pathway[43]. Increased plasma CXCL9 has been shown previously in GCA and is associated
625 with CXCR3+ cell infiltration into diseased arteries[44]. Previous studies speculated that TAK
626 and GCA differ in the susceptibility of T-cell pathways to glucocorticoids whereby Th1
627 responses persist in GCA and Th17 responses persist in TAK after treatment initiation[45,46].
628 Our observation that CXCL9 was exclusively increased in GCA while IL17A was exclusively
629 increased in TAK may support this theory.
630
631 Beyond comparing LVV types, this study provided several disease-specific insights. We
632 identified novel markers of active disease in TAK and in LV-GCA. Disease activity assessment
633 is challenging in LVV, where existing markers like CRP have well-recognised limitations and
634 there can be practical constraints regarding the frequent use of vascular imaging[7,8]. In a proof-
635 of-principle analysis, we demonstrate that a single additional marker, the ECM glycoprotein
636 COMP, used in combination with CRP markedly increases the accuracy of disease activity
637 detection when compared to the use of CRP alone. Although further study is required to
638 validate the novel markers identified here in independent cohorts, our findings suggest that
639 significant improvements can be made toward this important challenge with simple additions
640 to the laboratory testing regimes used for monitoring LVV. Importantly, we also found that
641 many proteins remained altered in TAK and LV-GCA patients despite clinically quiescent
642 disease. OSM and AXIN1 were elevated regardless of disease activity while activity markers
643 like S100A12 and VEGFA were highest in active disease but remained increased despite
644 clinical disease quiescence. These findings may parallel the inaccuracy of clinical disease
645 activity assessment compared to histopathological or radiological evaluations of arterial
646 inflammation[47–49]. However, we observed similar derangements in TAK patients who had
647 achieved durable clinical remission (defined here as the absence of any symptom, sign,
648 laboratory feature or radiographic evidence for active TAK over last 3 years of monitoring and
649 the safe cessation of all immunosuppressive treatments). Therefore, while the persistent
650 changes observed likely indicate subclinical inflammation, future studies are required to
651 determine whether their association with clinically important outcomes.

652
653 Our results suggest that biopsy-positive and negative C-GCA are proteomically distinct. There
654 are two possibilities that could explain our findings. First, despite a careful clinical phenotyping
655 algorithm which included external expert review, there may be instances of misclassification
656 within the TAB- C-GCA group, such that some patients were erroneously labelled as C-GCA.
657 However, this cannot fully explain our findings since the TAB- C-GCA group included some
658 patients with a positive USS. Alternatively, TAB positivity may reflect the burden of arterial
659 disease. Skip lesions, with discontinuous segments of arterial inflammation, can occur in GCA
660 and so a patient with lower burden of arterial disease is more likely to have a negative biopsy
661 on the small biopsy section of artery sampled. Thus, it is possible that the proteomic read-out
662 may reflect quantitative differences in the extent of arteritis. Our clinical lab data provided
663 additional evidence of differences between TAB+ and TAB- patients, with higher ESR, CRP
664 and platelet count in the former group, in keeping with previous studies[50–52]. Other clinical
665 differences in TAB+ and TAB- C-GCA have been described, including greater risk of visual
666 loss[52,53] and higher prevalence of PMR in TAB+ patients[50], although these findings have not
667 replicated in all case series[54]. Our data support the concept that C-GCA can be stratified by
668 biopsy into biologically distinct endotypes, which may have implications for future trial design
669 and precision medicine strategies.
670
671 Our study had limitations. We used a targeted proteomic panel which was enriched for
672 inflammatory and vascular proteins and thus our ability to compare between LVV groups is
673 limited to the proteins measured. The HCs in Cohort 1 were well-matched to TAK patients but
674 were younger than LV-GCA patients. Differences in study design between Cohort 1 and
675 Cohort 2 mean that proteomic differences between C-GCA and the other LVV groups may be
676 confounded by differences in disease duration and treatment history. In addition, the controls
677 in Cohort 2 (“Not GCA”) were individuals who presented with symptoms for which a diagnosis
678 of C-GCA was considered but ultimately excluded, whereas the controls in Cohort 1 were
679 healthy participants with no symptoms. In Cohort 1, there was heterogeneity in treatment, with
680 varying use of steroids and other immunosuppressants which could potentially impact the
681 plasma proteome. However, treatment (particularly glucocorticoid dose) is given in response
682 to disease activity, reflected in the correlation between disease activity scores and
683 prednisolone dose in Cohort 1. Thus attempting to statistically adjust for treatment risks over-
684 adjustment[55,56]. For supervised learning, we split the data into training and test sets but the
685 relatively modest sample sizes mean that estimates of model performance are more
686 vulnerable to stochastic variation. We mitigated this by also estimating model performance
687 through cross-validation in the larger training set. Finally, in the case of membrane-bound
688 proteins that undergo cleavage to produce a soluble form, it is not always clear whether

689 plasma protein measurements are exclusively capturing the latter or also protein from cell
690 membranes (for example, arising from *in vivo* sources such as exo-/ectosomes or *ex vivo*
691 processes such as venepuncture or sample processing), complicating interpretation.
692
693 In conclusion, similarities in the plasma proteomic profiles of active TAK and GCA indicate
694 common effector pathways resulting in inflammatory arterial damage despite differences in
695 genetic aetiology. Our integrated analysis of plasma and arterial tissue highlight the role
696 played by macrophages and their protein products in LVV and indicate significant potential for
697 their targeting in novel treatments and biomarkers. Future work should expand the molecular
698 characterisation of the LVV disease spectrum by extending the number of proteins measured
699 via use of complementary proteomic platforms and by concurrent measurement of other -omic
700 layers (e.g. RNA-seq of immune cells). Longitudinal studies characterising the temporal
701 changes in the molecular profile across the disease course will be valuable in delineating acute
702 from chronic changes and allowing intra-individual assessment of putative biomarkers
703 identified here.

704 # Main Figure Legends

705

706 **Figure 1. Study Overview.**

707 *Schematic overview of study to investigate the plasma proteomic changes associated with each form*
708 *of large-vessel vasculitis in two independent cohorts. Cohort 1: patients with established Takayasu*
709 *arteritis (TAK) and large-vessel giant cell arteritis (LV-GCA) and healthy control (HC) participants.*
710 *Cohort 2: patients presenting acutely with possible cranial giant cell arteritis in whom the diagnosis was*
711 *subsequently confirmed (C-GCA) or ruled out (Not C-GCA). Disease-specific proteomic profiles defined*
712 *by differential abundance analysis were compared. Network-based analysis of LVV-associated proteins*
713 *and integrated analysis with published tissue and cell-type datasets was also conducted.*

714

715 **Figure 2. Plasma proteomic changes in TAK and LV-GCA compared to Healthy Control**
716 **participants**

717 *Volcano plots showing results of differential protein abundance analyses: A) Takayasu Arteritis patients*
718 *(TAK, N=96) vs healthy controls (HC, N=35) B) Large-Vessel Giant Cell Arteritis (LV-GCA, N=35) vs*
719 *HC. -Log10(P_{adj}) = -$\log_{10}$ Benjamini-Hochberg adjusted p-value. Red and blue indicate proteins that are*
720 *significantly ($P_{adj} < 0.05$) upregulated and downregulated, respectively. C) Venn diagram showing the*
721 *overlap in proteins significantly altered in TAK vs HC compared to LV-GCA vs HC analyses. D)*
722 *Comparison of $\log_2$ fold changes in all proteins for TAK vs HC and LV-GCA vs HC analyses, diagonal*
723 *lines represent line of identity and +/- 0.5 $\log_2$ fold change. Blue = proteins significant in both analyses;*
724 *orange = significant only in TAK vs HC; teal = significant only in LV-GCA vs HC; grey = non-significant*
725 *in both analyses. E) Violin plots showing scaled protein levels (as Z-scores) for example proteins with*
726 *prominent changes in both TAK and LV-GCA. $P_{adj} < 0.05$: *, $P \leq 0.01$: **, $P \leq 0.001$: ***, $P \leq 0.0001$:*
727 *****.*

728

729 **Figure 3. Proteins associated with active disease within TAK and LV-GCA patients**

730 *A) Points indicating log_2 fold change estimate +/- standard error (horizontal bars) for proteins that were*
731 *significantly (adjusted $P < 0.05$) differentially abundant in the active vs inactive patient analysis for*
732 *Takayasu Arteritis only (TAK, N=56 vs N=40) (top panel), both diseases (middle panel) and Large-*
733 *Vessel Giant Cell Arteritis only (LV-GCA, N=11 vs N=24) (bottom panel). B) Functional categories of*
734 *differentially abundant proteins from TAK and LV-GCA activity analyses. Violin plots depict the scaled*
735 *abundance values (Z-scores) for proteins associated with disease activity in both diseases (C) and for*
736 *the proteins which had divergent associations with disease activity in TAK and LV-GCA (D & E). P-*
737 *values adjusted using Benjamini-Hochberg method; No symbol: non-significant, adjusted $P < 0.05$: *, P*
738 *≤ 0.01: **, $P \leq 0.001$: ***.*

739

740 **Figure 4. Proteomic changes associated with C-GCA are most pronounced in biopsy**
741 **proven disease**

742 *A) Volcano plots for the differential protein abundance comparisons of Cranial Giant Cell Arteritis (C-*
743 *GCA, N=150) cases vs Not C-GCA cases (N=89) and B) for the comparison of temporal artery biopsy*
744 *positive C-GCA (C-GCA TAB+, N=56) versus Not C-GCA (N=89).* $-Log_{10}(P_{adj}) = -log_{10}$ *Benjamini-*
745 *Hochberg adjusted p-value. Red and blue indicate proteins that are significantly* ($P_{adj} < 0.05$)
746 *upregulated and downregulated, respectively. C) Boxplot showing comparison of C-reactive protein*
747 *(CRP), erythrocyte sedimentation rate (ESR) and platelet count between Not C-GCA, C-GCA TAB- and*
748 *C-GCA TAB+ patients. Median and IQR represented by line and box edges respectively, upper whisker*
749 *represents the upper quartile plus 1.5 times the IQR, lower whisker represents lower quartile minus 1.5*
750 *times IQR. Statistical comparisons made with Kruskal-Wallis and Dunn's post-hoc tests. D)*
751 *Comparison of* log_2 *fold changes for differentially abundant proteins in C-GCA TAB+ vs Not C-CGA and*
752 *C-GCA TAB- vs Not C-GCA, diagonal line represents line of identity. E) Functional categories of*
753 *differentially abundant proteins in C-GCA TAB+ vs Not C-GCA comparison. F) Violin plots showing*
754 *scaled protein levels (Z-score) for example proteins with prominent changes in C-GCA TAB+ cases.*
755 *NS: non-significant, adjusted P < 0.05: *, P ≤ 0.0001: ****.*

756

757 **Figure 5. Comparison of active TAK, LV-GCA and biopsy-proven C-GCA proteomic**
758 **profiles**

759 *A) Heatmap showing* log_2 *fold changes (FC) of the 112 differentially abundant proteins (DAP) identified*
760 *in active Takayasu Arteritis (TAK) vs healthy control (HC), active Large-Vessel Giant Cell Arteritis (LV-*
761 *GCA) vs HC and temporal artery biopsy positive (TAB+) C-GCA vs Not C-GCA comparisons. Left: navy*
762 *boxes represent proteins with statistically significant changes (Adjusted P < 0.05) in each disease.*
763 *Right: annotated functional category for each protein. B) Comparison of disease* Log_2 *FC for 112 DAP,*
764 *diagonal lines represent the line of identity. Network plots of (C), known protein-protein interactions and*
765 *(D), protein-protein co-expression for proteins with concordant changes in each disease (74). Node size*
766 *corresponds to number of edges. For C, high confidence interactions (≥0.9) were sourced from*
767 *STRING*[18] *and for D, protein co-expression was defined as a Pearson correlation ≥0.6 in both active*
768 *TAK/LV-GCA patients and TAB+ C-GCA patients. E) Violin plots showing scaled abundance values (Z-*
769 *scores) for selected proteins associated with active TAK and LV-GCA but not C-GCA (F) and those*
770 *identified as different between active LV-GCA and C-GCA vs active TAK. P-values adjusted using*
771 *Benjamini-Hochberg method; No symbol: non-significant, Adjusted P < 0.05: *, P ≤ 0.01: **, P ≤ 0.001:*
772 ****, P ≤ 0.0001: *****

773

774 **Figure 6. Correspondence of LVV plasma profile to arterial tissue phenotype**

775 *Comparison of plasma proteomic profiles associated with LVV and gene expression changes identified*
776 *in aortic tissue affected by large-vessel vasculitis (LVV)*[22]*. A) Pie chart showing the proportion of 112*
777 *LVV-associated plasma proteins (Supplementary Data 18) that were also differentially expressed*
778 *(Adjusted $P < 0.05$) in the comparison of large-vessel giant cell arteritis (LV-GCA) related aortic*
779 *aneurysm (N=8) to non-inflammatory aortic aneurysm (NI-AA) by bulk RNA-seq (N=25). B) Comparison*
780 *of plasma protein and aortic gene expression log_2 fold changes (Log_2FC) for the 47 proteins and*
781 *corresponding genes that had significant changes in both LVV plasma and aortic tissue, each point*
782 *represents a gene/protein pair. For proteomics (Y axes), Log_2FCs represent active Takayasu Arteritis*
783 *(TAK) vs healthy control (HC), active LV-GCA vs HC and temporal artery biopsy positive cranial-GCA*
784 *(TAB+ C-GCA) vs Not C-GCA comparisons. For transcriptomics (X axes), Log_2FCs represent LV-GCA*
785 *associated aortitis vs NI-AA. (C-E), Dot plots showing aortic gene expression of genes/proteins DA in*
786 *both LVV plasma and aortic tissue. Genes proteins typically expressed by macrophages (C), non-*
787 *haematopoietic stromal cells (D) and lymphocytes (E). Gene expression measured in transcripts per*
788 *million (TPM), cell-type expression classified using blueprint data (Figure S8). P-values were adjusted*
789 *using Benjamini-Hochberg method.*

790 ## Acknowledgments

791 We thank Prof. Marina Botto and Prof. Matthew Pickering for helpful comments on the
792 manuscript. We thank the patients and healthy volunteers who participated in this study, along
793 with the clinical research teams who recruited patients. We thank Surjeet Singh as the chief
794 study coordinator for TABUL, and Bhaskar Dasgupta as a co-investigator on TABUL who
795 played a leading role in the study recruitment. Prof Mason tragically passed away during the
796 study and we dedicate this paper to his memory.

797

798 ## Supplemental Material

799 **Supplementary Information File.docx**

800 Supplementary Methods

801 Supplementary Table 1: TAK and LV-GCA cohorts

802 Supplementary Table 2: C-GCA cohort

803 Supplementary Table 3. Performance of predictive models for discrimination of biopsy-proven
804 C-GCA from Not C-GCA

805 Supplementary Table 4: Confusion matrix comparing model predictions from the 11-protein
806 LASSO model in the Test set versus true labels

807 Figure S1. Comparing TAK findings to those of a previous plasma proteomic study

808 Figure S2. TAK and LV-GCA vs HC comparison

809 Figure S3. Plasma protein differences between TAK and LV-GCA patients

810 Figure S4. Proteins associated with Disease Activity Score in TAK

811 Figure S5. Novel markers provide improved detection of disease activity compared to CRP
812 alone in TAK

813 Figure S6. Differentially abundant proteins in inactive TAK & LV-GCA

814 Figure S7. Proteomic changes in C-GCA are most pronounced in biopsy proven disease

815 Figure S8. Comparison of proteomic changes in TAB+ and TAB- C-GCA patients

816 Figure S9. Comparing biopsy proven C-GCA findings to those of a previous plasma proteomic
817 study

818 Figure S10. Supervised learning to identify diagnostic markers of biopsy-proven C-GCA

819 Figure S11. Tissue expression of LVV-associated plasma proteins

820 Figure S12. Cell-type expression profile of proteins/genes identified as dysregulated in both
821 LVV plasma and tissue

822 **Supplementary Data File.xlsx**

823 Supplementary Data 1: Proteins measured in this study

824 Supplementary Data 2: Pathway enrichment of proteins measured in this study

825 Supplementary Data 3: Characteristics of TAK and LV-GCA patients with inactive and active
826 disease

827 Supplementary Data 4: Differential protein abundance analysis TAK vs HC

828 Supplementary Data 5: Differential protein abundance analysis LV-GCA vs HC

829 Supplementary Data 6: Differential protein abundance analysis TAK vs LV-GCA

830 Supplementary Data 7: Differential protein abundance analysis Active TAK vs Inactive TAK

831 Supplementary Data 8: Differential protein abundance analysis Active LV-GCA vs Inactive LV-
832 GCA

833 Supplementary Data 9: Differential protein abundance analysis Inactive TAK vs HC

834 Supplementary Data 10: Differential protein abundance analysis Inactive LV-GCA vs HC

835 Supplementary Data 11: Characteristics of TAK patients in durable clinical remission

836 Supplementary Data 12: Differential protein abundance analysis C-GCA vs Not C-GCA

837 Supplementary Data 13: Differential protein abundance analysis C-GCA TAB+ vs Not C-GCA

838 Supplementary Data 14: Differential protein abundance analysis C-GCA TAB- vs Not C-GCA

839 Supplementary Data 15: Characteristics of Not C-GCA cases and C-GCA patients stratified
840 by TAB result

841 Supplementary Data 16: Differential protein abundance analysis Active TAK vs HC

842 Supplementary Data 17: Differential protein abundance analysis Active LV-GCA vs HC

843 Supplementary Data 18: Comparison of active TAK, active LV-GCA and C-GCA TAB+
844 proteomic profiles

845 Supplementary Data 19: Proteins & Genes dysregulated in both LVV plasma and arterial
846 tissue

847 # References

848 1. Pugh D, Karabayas M, Basu N, Cid MC, Goel R, Goodyear CS, et al. Large vessel
849 vasculitis. Nat Rev Dis Primer. 2022 Jan 6;7(1):93.

850 2. Koster MJ, Matteson EL, Warrington KJ. Large-vessel giant cell arteritis: diagnosis,
851 monitoring and management. Rheumatology. 2018 Feb 1;57(suppl_2):ii32–42.

852 3. Gribbons KB, Ponte C, Carette S, Craven A, Cuthbertson D, Hoffman GS, et al. Patterns
853 of Arterial Disease in Takayasu Arteritis and Giant Cell Arteritis. Arthritis Care Res.
854 2020;72(11):1615–24.

855 4. Grayson PC. Lumpers and Splitters: Ongoing Issues in the Classification of Large Vessel
856 Vasculitis. J Rheumatol. 2015 Feb 1;42(2):149–51.

857 5. Maksimowicz-McKinnon K, Clark TM, Hoffman GS. Takayasu arteritis and giant cell
858 arteritis: a spectrum within the same disease? Medicine (Baltimore). 2009 Jul;88(4):221–
859 6.

860 6. Watanabe Y, Miyata T, Tanemoto K. Current Clinical Features of New Patients With
861 Takayasu Arteritis Observed From Cross-Country Research in Japan. Circulation. 2015
862 Nov 3;132(18):1701–9.

863 7. Tombetti E, Hysa E, Mason JC, Cimmino MA, Camellino D. Blood Biomarkers for
864 Monitoring and Prognosis of Large Vessel Vasculitides. Curr Rheumatol Rep. 2021 Feb
865 10;23(3):17.

866 8. O'Connor TE, Carpenter HE, Bidari S, Waters MF, Hedna VS. Role of inflammatory
867 markers in Takayasu arteritis disease monitoring. BMC Neurol. 2014 Mar 28;14:62.

868 9. Broder MS, Sarsour K, Chang E, Collinson N, Tuckwell K, Napalkov P, et al.
869 Corticosteroid-related adverse events in patients with giant cell arteritis: A claims-based
870 analysis. Semin Arthritis Rheum. 2016 Oct 1;46(2):246–52.

871 10. Pujades-Rodriguez M, Morgan AW, Cubbon RM, Wu J. Dose-dependent oral
872 glucocorticoid cardiovascular risks in people with immune-mediated inflammatory
873 diseases: A population-based cohort study. PLOS Med. 2020 Dec 3;17(12):e1003432.

874 11. Joshi A, Rienks M, Theofilatos K, Mayr M. Systems biology in cardiovascular disease: a
875 multiomics approach. Nat Rev Cardiol. 2021 May;18(5):313–30.

876 12. Grayson PC, Ponte C, Suppiah R, Robson JC, Gribbons KB, Judge A, et al. 2022
877 American College of Rheumatology/EULAR Classification Criteria for Takayasu Arteritis.
878 Arthritis Rheumatol. 2022;74(12):1872–80.

879 13. Stone JH, Tuckwell K, Dimonaco S, Klearman M, Aringer M, Blockmans D, et al. Trial of
880 Tocilizumab in Giant-Cell Arteritis. N Engl J Med. 2017 Jul 27;377(4):317–28.

881 14. Misra R, Danda D, Rajappa SM, Ghosh A, Gupta R, Mahendranath KM, et al.
882 Development and initial validation of the Indian Takayasu Clinical Activity Score
883 (ITAS2010). Rheumatol Oxf Engl. 2013 Oct;52(10):1795–801.

884 15. Kerr GS, Hallahan CW, Giordano J, Leavitt RY, Fauci AS, Rottem M, et al. Takayasu
885 arteritis. Ann Intern Med. 1994 Jun 1;120(11):919–29.

886 16. Hellmich B, Agueda A, Monti S, Buttgereit F, de Boysson H, Brouwer E, et al. 2018
887 Update of the EULAR recommendations for the management of large vessel vasculitis.
888 Ann Rheum Dis. 2020 Jan;79(1):19–30.

889 17. Luqmani R, Lee E, Singh S, Gillett M, Schmidt WA, Bradburn M, et al. The Role of
890 Ultrasound Compared to Biopsy of Temporal Arteries in the Diagnosis and Treatment of
891 Giant Cell Arteritis (TABUL): a diagnostic accuracy and cost-effectiveness study. Health
892 Technol Assess Winch Engl. 2016 Nov;20(90):1–238.

893 18. Szklarczyk D, Kirsch R, Koutrouli M, Nastou K, Mehryary F, Hachilif R, et al. The STRING
894 database in 2023: protein-protein association networks and functional enrichment
895 analyses for any sequenced genome of interest. Nucleic Acids Res. 2023 Jan
896 6;51(D1):D638–46.

897 19. Csárdi G, Nepusz T. The igraph software package for complex network research. In 2006
898 [cited 2024 Jul 11]. Available from: https://www.semanticscholar.org/paper/The-igraph-
899 software-package-for-complex-network-Cs%C3%A1rdi-
900 Nepusz/1d2744b83519657f5f2610698a8ddd177ced4f5c

901 20. Lonsdale J, Thomas J, Salvatore M, Phillips R, Lo E, Shad S, et al. The Genotype-Tissue
902 Expression (GTEx) project. Nat Genet. 2013 Jun;45(6):580–5.

903 21. Uhlén M, Fagerberg L, Hallström BM, Lindskog C, Oksvold P, Mardinoglu A, et al. Tissue-
904 based map of the human proteome. Science. 2015 Jan 23;347(6220):1260419.

905 22. Hur B, Koster MJ, Jang JS, Weyand CM, Warrington KJ, Sung J. Global Transcriptomic
906 Profiling Identifies Differential Gene Expression Signatures between Inflammatory and
907 Non-inflammatory Aortic Aneurysms. Arthritis Rheumatol Hoboken NJ. 2022
908 Aug;74(8):1376–86.

909 23. Chen Y, Lun ATL, Smyth GK. From reads to genes to pathways: differential expression
910 analysis of RNA-Seq experiments using Rsubread and the edgeR quasi-likelihood
911 pipeline. F1000Research. 2016 Aug 2;5:1438.

912 24. Friedman JH, Hastie T, Tibshirani R. Regularization Paths for Generalized Linear Models
913 via Coordinate Descent. J Stat Softw. 2010 Feb 2;33:1–22.

914 25. Kuhn M. Building Predictive Models in R Using the caret Package. J Stat Softw. 2008
915 Nov 10;28:1–26.

916 26. Cui X, Qin F, Song L, Wang T, Geng B, Zhang W, et al. Novel Biomarkers for the
917 Precisive Diagnosis and Activity Classification of Takayasu Arteritis. Circ Genomic Precis
918 Med. 2019 Jan;12(1):e002080.

919 14. Robinette ML, Rao DA, Monach PA. The Immunopathology of Giant Cell Arteritis Across
920 Disease Spectra. Front Immunol. 2021 Feb 25

921 28. Burja B, Feichtinger J, Lakota K, Thallinger GG, Sodin-Semrl S, Kuret T, et al. Utility of
922 serological biomarkers for giant cell arteritis in a large cohort of treatment-naïve patients.
923 Clin Rheumatol. 2019 Feb 1;38(2):317–29.

924 29. Fernández JM, de la Torre V, Richardson D, Royo R, Puiggròs M, Moncunill V, et al. The
925 BLUEPRINT Data Analysis Portal. Cell Syst. 2016 Nov 23;3(5):491-495.e5.

926 30. Ponte C, Grayson PC, Robson JC, Suppiah R, Gribbons KB, Judge A, et al. 2022
927 American College of Rheumatology/EULAR Classification Criteria for Giant Cell Arteritis.
928 Arthritis Rheumatol. 2022;74(12):1881–9.

929 31. Carmona FD, Coit P, Saruhan-Direskeneli G, Hernández-Rodríguez J, Cid MC, Solans
930 R, et al. Analysis of the common genetic component of large-vessel vasculitides through
931 a meta-Immunochip strategy. Sci Rep. 2017 Mar 9;7:43953.

932 32. Kong X, Xu M, Cui X, Ma L, Cheng H, Hou J, et al. Potential Role of Macrophage
933 Phenotypes and CCL2 in the Pathogenesis of Takayasu Arteritis. Front Immunol. 2021
934 May 17;12:646516.

935 33. Jiemy WF, van Sleen Y, van der Geest KS, ten Berge HA, Abdulahad WH, Sandovici M,
936 et al. Distinct macrophage phenotypes skewed by local granulocyte macrophage colony-
937 stimulating factor (GM-CSF) and macrophage colony-stimulating factor (M-CSF) are
938 associated with tissue destruction and intimal hyperplasia in giant cell arteritis. Clin
939 Transl Immunol. 2020 Aug 27;9(9):e1164.

940 34. Aloufi NA, Ali AK, Burke Schinkel SC, Molyer B, Barros PO, McBane JE, et al. Soluble
941 CD127 potentiates IL-7 activity in vivo in healthy mice. Immun Inflamm Dis.
942 2021;9(4):1798–808.

943 35. Yoon T, Pyo JY, Ahn SS, Song JJ, Park YB, Lee SW. Serum soluble interleukin-7
944 receptor alpha levels are negatively correlated with the simultaneous activity of
945 antineutrophil cytoplasmic antibody-associated vasculitis. Clin Exp Rheumatol. 2023
946 Apr;41(4):879–86.

947 36. Lundtoft C, Afum-Adjei Awuah A, Rimpler J, Harling K, Nausch N, Kohns M, et al.
948 Aberrant plasma IL-7 and soluble IL-7 receptor levels indicate impaired T-cell response
949 to IL-7 in human tuberculosis. PLoS Pathog. 2017 Jun 5;13(6):e1006425.

950 37. Meyer A, Parmar PJ, Shahrara S. Significance of IL-7 and IL-7R in RA and autoimmunity.
951 Autoimmun Rev. 2022 Jul 1;21(7):103120.

952 38. Sato Y, Jain A, Ohtsuki S, Okuyama H, Sturmlechner I, Takashima Y, et al. Stem-like
953 CD4+ T cells in perivascular tertiary lymphoid structures sustain autoimmune vasculitis.
954 Sci Transl Med. 2023 Sep 6;15(712):eadh0380.

955 39. Ware CF, Croft M, Neil GA. Realigning the LIGHT signaling network to control
956 dysregulated inflammation. J Exp Med. 2022 May 23;219(7):e20220236.

957 40. Shaikh RB, Santee S, Granger SW, Butrovich K, Cheung T, Kronenberg M, et al.
958 Constitutive Expression of LIGHT on T Cells Leads to Lymphocyte Activation,
959 Inflammation, and Tissue Destruction. J Immunol. 2001 Dec 1;167(11):6330–7.

960 41. Herro R, Croft M. The control of tissue fibrosis by the inflammatory molecule LIGHT (TNF
961 Superfamily member 14). Pharmacol Res. 2016 Feb;104:151–5.

962 42. Golledge J, Clancy P, Maguire J, Lincz L, Koblar S. The role of tenascin C in
963 cardiovascular disease. Cardiovasc Res. 2011 Oct 1;92(1):19–28.

964 43. Berthoud TK, Dunachie SJ, Todryk S, Hill AVS, Fletcher HA. MIG (CXCL9) is a more
965 sensitive measure than IFN-γ of vaccine induced T-cell responses in volunteers receiving
966 investigated malaria vaccines. J Immunol Methods. 2009 Jan 1;340(1):33–41.

967 44. Graver JC, Abdulahad W, van der Geest KSM, Heeringa P, Boots AMH, Brouwer E, et
968 al. Association of the CXCL9-CXCR3 and CXCL13-CXCR5 axes with B-cell trafficking in
969 giant cell arteritis and polymyalgia rheumatica. J Autoimmun. 2021 Sep;123:102684.

970 45. Deng J, Younge BR, Olshen RA, Goronzy JJ, Weyand CM. Th17 and Th1 T-cell
971 responses in giant cell arteritis. Circulation. 2010 Feb 23;121(7):906–15.

972 46. Saadoun D, Garrido M, Comarmond C, Desbois AC, Domont F, Savey L, et al. Th1 and
973 Th17 cytokines drive inflammation in Takayasu arteritis. Arthritis Rheumatol Hoboken
974 NJ. 2015 May;67(5):1353–60.

975 47. Kaymakci MS, Boire NA, Bois MC, Elfishawi MM, Langenfeld HE, Hanson AC, et al.
976 Persistent aortic inflammation in patients with giant cell arteritis. Autoimmun Rev. 2023
977 Sep;22(9):103411.

978 48. Uy CP, Tarkin JM, Gopalan D, Barwick TD, Tombetti E, Youngstein T, et al. The Impact
979 of Integrated Noninvasive Imaging in the Management of Takayasu Arteritis. JACC
980 Cardiovasc Imaging. 2021 Feb;14(2):495–500.

981 49. Grayson PC, Alehashemi S, Bagheri AA, Civelek AC, Cupps TR, Kaplan MJ, et al.
982 Positron Emission Tomography as an Imaging Biomarker in a Prospective, Longitudinal
983 Cohort of Patients with Large Vessel Vasculitis. Arthritis Rheumatol Hoboken NJ. 2018
984 Mar;70(3):439–49.

985 50. Koster MJ, Yeruva K, Crowson CS, Muratore F, Labarca C, Warrington KJ. Giant cell
986 arteritis and its mimics: A comparison of three patient cohorts. Semin Arthritis Rheum.
987 2020 Oct;50(5):923–9.

988 51. Gonzalez-Gay MA, Garcia-Porrua C, Llorca J, Gonzalez-Louzao C, Rodriguez-Ledo P.
989 Biopsy-negative giant cell arteritis: Clinical spectrum and predictive factors for positive
990 temporal artery biopsy. Semin Arthritis Rheum. 2001 Feb 1;30(4):249–56.

991 52. Duhaut P, Pinède L, Bornet H, Demolombe-Ragué S, Dumontet C, Ninet J, et al. Biopsy
992 proven and biopsy negative temporal arteritis: differences in clinical spectrum at the
993 onset of the disease. Ann Rheum Dis. 1999 Jun 1;58(6):335–41.

994 53. Chatelain D, Duhaut P, Schmidt J, Loire R, Bosshard S, Guernou M, et al. Pathological
995 features of temporal arteries in patients with giant cell arteritis presenting with permanent
996 visual loss. Ann Rheum Dis. 2009 Jan 1;68(1):84–8.

997 54. Putman MS, Gribbons KB, Ponte C, Robson J, Suppiah R, Craven A, et al.
998 Clinicopathologic Associations in a Large International Cohort of Patients With Giant Cell
999 Arteritis. Arthritis Care Res. 2022 Jun;74(6):1013–8.

1000 55. Westreich D, Greenland S. The Table 2 Fallacy: Presenting and Interpreting Confounder
1001 and Modifier Coefficients. Am J Epidemiol. 2013 Feb 15;177(4):292–8.

1002 56. Schisterman EF, Cole SR, Platt RW. Overadjustment Bias and Unnecessary Adjustment
1003 in Epidemiologic Studies. Epidemiol Camb Mass. 2009 Jul;20(4):488–95.

1004